

SEPARATION AND THERMAL MODIFICATION OF MONTMORILLONITE FROM TANAH DATAR CLAY AND ITS CATALYTIC APPLICATION IN BIODIESEL PRODUCTION FROM WASTE FRYING OILS

ZARNIDA WIDIA NENGSIH¹; RAHAYU RAHAYU¹; SYUKRI ARIEF¹; UPITA SEPTIANI¹;
MATLAL FAJRI ALIF¹ and SYUKRI SYUKRI^{1*}

ABSTRACT

Natural clay comprises a blend of diverse minerals exhibiting distinct structures and characteristics. Montmorillonite exhibits strong acidity and stabilising effects on active species due to its unique layered structure, thus making it a suitable material for use as a heterogeneous catalyst. Therefore, this research aims to examine the effect of separation and thermal modification process of Tanah Datar clay minerals, as well as their catalytic activity in the conversion of waste frying oil (WFO) into biodiesel. The catalysts were evaluated using X-ray diffraction (XRD), X-ray fluorescence (XRF) and Laser Particle Size Analyser (LPSA). The uncalcined clay primarily consists of montmorillonite, along with kaolinite, hematite and quartz. Upon calcination, montmorillonite transforms into meta montmorillonite. The particle size of montmorillonite increases after separation and calcination. The catalysts were employed in a lab-scale biodiesel production via transesterification reaction, employing a mole ratio of oil and methanol of 1:6, catalyst amount of 3.00% (w/w), stirring speed of 500 rpm, and a temperature of 70°C for 3 hr. Both uncalcined and calcined montmorillonite catalysts can enhance biodiesel yield by up to 80.11%. This observation demonstrates the considerable potential of the implemented treatment as a catalyst in biodiesel production.

Keywords: biodiesel, catalyst, clay, montmorillonite, transesterification.

Received: 27 November 2023; **Accepted:** 20 June 2024; **Published online:** 2 September 2024.

INTRODUCTION

Energy is one of the factors in sustaining human life activities. Energy consumption always increases every year. Continuous energy use results in a shortage of energy originating from fossil fuels. The use of fossil fuels is also a global problem due to excessive levels of CO₂ emissions, environmental

impacts and threats to the economy, environment, and human welfare (Azni et al., 2023; Rehman et al., 2021). One renewable energy source that can lessen the scarcity of fossil fuels and lessen environmental pollution is biodiesel (Pacheco-López et al., 2021; Pikula et al., 2020). Biodiesel fuel can replace fossil fuels used for diesel engines. It is more attractive than diesel fuel because it is non-toxic, biodegradable, and can be produced from renewable sources, making it a sustainable alternative fuel (Nguyen et al., 2023; Siddeg et al., 2022). Additionally, it can also help reduce greenhouse gas emissions by up to 86% compared to petroleum diesel (Suwarno et al., 2021; Xu et al.,

¹ Chemistry Department,
Faculty of Mathematics and Natural Sciences,
Universitas Andalas, Limau Manis Campus,
Padang, 25163 Indonesia.

* Corresponding author e-mail: syukridarajat@sci.unand.ac.id

2022). It can be made through several methods, such as dilution, pyrolysis, microemulsion, and transesterification (Irawan et al., 2021; Mishra & Goswami, 2018; Supriyanto et al., 2021). The transesterification method is preferred for biodiesel due to its low cost compared to other methods. In addition, the transesterification process is also relatively simple (Gouran et al., 2021; Salaheldeen et al., 2021).

Making biodiesel by transesterification method uses raw materials containing triglycerides, such as vegetable oils. Some types of vegetable oils that have been used are sunflower (Jabbari, 2018; Khan et al., 2023; Vital-López et al., 2023), castor oil (Bibin et al., 2020; Mustafa et al., 2023; Ubaid et al., 2022), coconut oil (Bambase et al., 2021; Lugo-Méndez et al., 2021), and palm oil (Nang et al., 2009; Palaniselvam et al., 2023; Syukri et al., 2022). However, the use of waste frying oil (WFO) is of great interest. This is because biodiesel from WFO is an environmentally friendly process. After all, WFO can be utilised, making it more economical and effective in waste management (Gouran et al., 2021; Sukkathanyawat & Wichianwat, 2023). The transesterification reaction also requires a catalyst. The catalysts used can be homogeneous catalysts and heterogeneous catalysts. Homogeneous catalysts have disadvantages such as difficulty in catalyst separation, high effluent generation (Pasae et al., 2021; Silva et al., 2015), and equipment corrosion, while heterogeneous catalysts offer advantages like reusability, selectivity, and low cost (Faruque et al., 2020; Gaide et al., 2023; Kibar et al., 2023). Therefore, many heterogeneous catalysts are now developed in the transesterification reaction, one of which is montmorillonite.

Montmorillonite belongs to the smectite group and has a 2:1 layer structure (Belghazdis & Hachem, 2022; Uddin, 2018; Yaghmaeiyan et al., 2022). Alumina and silica make up the majority of montmorillonite, a typical cationic clay; other metal oxides make up a small portion (Tripol'Skaya et al., 2009). Montmorillonite exhibits strong acidity and a stabilising effect on active species, such as metal nanoparticles, due to its unique layered structure. This makes it a suitable material for use as a heterogeneous catalyst (Takabatake & Motokura, 2022). Several studies have used montmorillonite as a catalyst for transesterification reactions, such as montmorillonite KST in producing biodiesel from palm oil (Kansedo et al., 2009), the novel modified montmorillonite to produce biodiesel from castor and *Jatropha* oil (Negm et al., 2017), and barium-loaded montmorillonite for the synthesis of biodiesel from waste cooking oil (WCO) (Sharma & Bhavani, 2021). Each of these reactions produces high yields of biodiesel. However, the chemical modification given to the montmorillonite catalyst requires

complicated steps and is expensive (Shapkin et al., 2017). Meanwhile, physical modifications can also be given to montmorillonite, such as thermal modifications (Abdrakhimova & Abdrakhimov, 2007; Wu et al., 2022). Previous researchers reported that clay calcined at 850°C could increase biodiesel yield (Admi et al., 2022).

The montmorillonite that is widely used in catalyst application is synthetic montmorillonite, which consequently increases production costs. However, montmorillonite is one of the minerals contained in natural clay. Separating montmorillonite from natural clay can be a solution to reduce catalyst production costs. Montmorillonite was separated from Boyolali natural clay by previous researchers and applied as an oil-bleaching agent (Taslimah et al., 2008). However, montmorillonite, separated from natural clay has never been used as a catalyst. Therefore, this research applies montmorillonite separated from natural clay as a catalyst in the transesterification reaction. Based on data in 2021, the availability of clay in Indonesia is very abundant. There are about 10,387.209 million tonnes of natural clay available in West Sumatera Province. Therefore, the catalyst raw material used in this study was taken from one of the areas in West Sumatera Province, namely Tanah Datar Regency because there have been no reports regarding the separation of montmorillonite minerals from clay in that area. The Tanah Datar area has abundant clay, which is characterised by the presence of brick production sites.

This study aims to determine the effect of separation process and thermal modification on mineral composition, physical and chemical properties of minerals, and catalytic activity of uncalcined and calcined montmorillonite from Tanah Datar clay in the process of converting WFO into biodiesel.

MATERIALS AND METHODS

Materials Preparation

The clays used in this study were taken from Andaleh, Batipuh District, Tanah Datar Regency, West Sumatra Province, Indonesia. The area is located at latitude 0°27'12.4"S and longitude 100°26'09.7"E in the form of a plateau area at an altitude of 946 m above sea level. The map of natural clay (*n-clay*) sampling locations can be seen in Figure 1. The *n-clay* was soaked in distilled water for 24 hr, filtered, and dried at 105°C for 3 hr. The clay was crushed and sieved with a sieve of 90 µm (Syukri et al., 2020). The heated clay (*h-clay*) catalyst was obtained ready to be separated from the montmorillonite mineral. The transesterification reaction was carried out following the methods

reported by previous researchers (Febiola et al., 2023) with some modifications using three times WFO and methanol (Merck) as raw materials. Ammonia hydroxide (NH₄OH) was used as a dispersing agent for montmorillonite from Tanah Datar clay following the method reported by previous researchers (Taslimah et al., 2008).

Separation and Thermal Modification of Montmorillonite

Montmorillonite was separated by dispersing it in an NH₄OH solution. In brief, 25 g of *h-clay* was stirred in 400 mL NH₄OH 2% (v/v) with a magnetic stirrer for 15 min and left for two days (Taslimah et al., 2008). The suspension was separated by centrifugation at 1,000 rpm for 5 min. The precipitate was separated and dried in an oven at 105°C to obtain the montmorillonite clay (*Mt-clay*) catalyst. Thermal modification is carried out by calcining the *Mt-clay* catalyst at a temperature of 850°C in a furnace for 4 hr to obtain the calcined montmorillonite clay (*c-Mt-clay*) catalyst.

Catalyst Characterisation

The catalyst's crystallinity was assessed through the utilisation of X-ray diffraction (XRD) equipment by X'Pert MPD (PANanalytical) which employed Cu Kα1 radiation (λ = 1.54059 Å). The equipment operated at 40 kV and 30 mA, covering an angular range of 2θ 10° to 90°. The oxide composition was determined using X-ray fluorescence (XRF) equipment by NEXCG Rigaku. Particle size was assessed using the Laser Particle Size Analyser (LPSA) equipment by Labtron, LLPA-C10, which has a measuring range of 0.01-2,000.00 μm.

Preparation and Determination of Free Fatty Acids in WFO

The preparation of WFO is done by heating it at 105°C until the water bubbles disappear. Free fatty acid (FFA) content was determined following the acid-base titration method reported by previous researchers (Febrianto et al., 2020) with the Equation (1):

$$\% \text{ FFA} = \frac{V_{\text{NaOH}} \times N_{\text{NaOH}} \times \text{Bm}_{\text{fatty acid}}}{M \times 1000} \quad (1)$$

where, V_{NaOH} is the volume of 0.1 N NaOH titration (in mL), N_{NaOH} is normality of NaOH, Bm_{fatty acid} is molecular weight of fatty acid (in g) and M is mass of oil sample.

Biodiesel Production Through Transesterification Reaction and Its Characterisation

The WFO used in this study has a density of 0.90 g cm⁻³ and FFA of 1.65%. The FFA value is lower than 3% so WFO can be used directly in the transesterification reaction. Each catalyst was used in the transesterification reaction of WFO by refluxing method. The molar ratio of WFO and methanol used was 1:6 with 3.00% (w/w) catalyst. The transesterification reaction was carried out for 3 hr at 70°C with a stirring speed of 500 rpm. The catalyst and glycerol were separated from the product mixture by centrifugation. The biodiesel layer was washed with 50°C aquadest at a volume of 1:1 and homogenised for 5 min. The mixture was allowed to stand so that the dense water would separate as the bottom layer and drained out. The remaining water in the biodiesel was removed



0°27'12.4"S 100°26'09.7"E

Figure 1. Map of natural clay sampling locations.

using anhydrous Na_2SO_4 . The yield of biodiesel was calculated using the Equation (2) (Munir et al., 2019):

$$\% \text{ Yield} = \frac{\text{Mass of biodiesel produced (g)}}{\text{Mass of oil used (g)}} \times 100 \quad (2)$$

Product Analysis

The type and content of methyl esters produced in biodiesel products are identified using Gas Chromatography-Mass Spectrometry/GC-MS (Shimadzu QP 2010 Ultra). The GC-MS instrument is equipped with a DB5 MS column with Helium as a carrier gas and an injection temperature of 250°C. The biodiesel product was determined for density at 15°C (ASTM D6751) and moisture content (ASTM D2709).

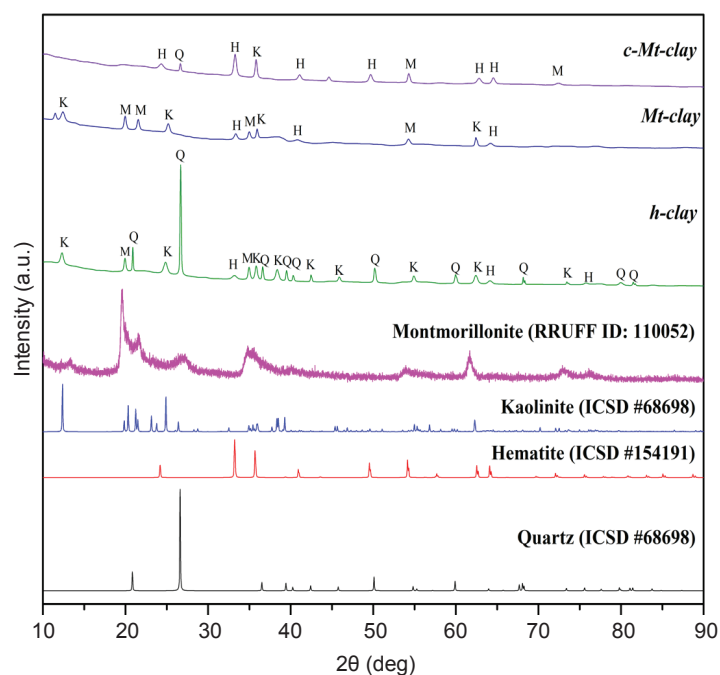
RESULTS AND DISCUSSION

X-ray Diffraction Characterisation

Figure 2 shows the X-ray diffraction pattern of the *h-clay*, *Mt-clay* and *c-Mt-clay* catalysts scanned at 2θ from 20°-90° that the Tanah Datar clay contains the minerals montmorillonite and kaolinite. The presence of montmorillonite (RRUFF ID: 110052) was found to have diffraction intensities at 2θ : 19.9° and 34.9°. Kaolinite in the *h-clay* sample was confirmed based on Inorganic

Crystal Structure Database (ICSD) No. 68698 with the appearance of diffraction intensity at 2θ : 12.3°; 24.8°; 36.5°; 38.3°; 42.4°; 45.8°; 54.8° and 62.3°. The presence of quartz (ICSD No. 68698) was found with high intensity at 2θ : 26.6°. Quartz is a stable phase of silica in the form of an inert compound. When at normal temperature, quartz has a trigonal quartz (α -quartz) structure (Götze et al., 2021). The diffraction intensity of hematite (ICSD No. 154191) was also found at 2θ : 33.1°; 36.5°; 64.0° and 75.7°.

The separation can cause changes in mineral peaks. Montmorillonite peaks appear at 2θ : 21.5° and 54.2°. Meanwhile, the peak that existed before separation remained after separation and there was an increase in intensity, namely at 19.9° and 34.9°. Kaolinite mineral as an impurity in *Mt-clay* also causes the disappearance of the peak at 2θ : 36.5°; 42.4°; 45.8° and 54.8°. Meanwhile, the kaolinite peak that is still present in the *Mt-clay* sample has a low intensity at 2θ : 12.4°; 25.1°; 35.9°; and 62.4°. Hematite also experiences peak loss at 2θ : 36.5° and 75.7°. The thermal modification given to *c-Mt-clay* caused the disappearance of most of the montmorillonite mineral peaks (Figure 2). Montmorillonite peaks were only found at 2θ : 54.2° and 72.5° with very low intensity. The diffraction peaks of *c-Mt-clay* are dominated by hematite peaks, at 2θ : 24.3°; 33.2°; 41.0°; 49.6°; 62.7° and 64.4°. Another interesting point is the appearance of a quartz peak at 2θ : 26.6° albeit with very low intensity, which was previously missing in the *Mt-clay* sample.



Note: M - montmorillonite, K - kaolinite, Q - quartz, H - hematite.

Figure 2. XRD diffratograms of *h-clay*, *Mt-clay*, and *c-Mt-clay*.

X-ray Fluorescence Characterisation

Thermal separation and modification affect the elemental and oxide composition of each catalyst (Table 1). According to the XRF analysis, it is evident that all catalyst samples contain a significant proportion of silicon (Si) and aluminium (Al) elements in their composition, whose levels reach more than 60% of the total of all elements in the sample. This shows that the catalysts used are indeed classified as clay because they have the main constituent composition of clay (Lomertwala et al., 2019). In addition, it can be seen that the type of montmorillonite contained in Tanah Datar clay is Ca-montmorillonite because there is Ca content in the clay (Park et al., 2016). Iron oxide occupies the third highest position as a constituent composition of clay catalysts whose levels reach 19%-32%. Determination of the Si/Al mole ratio on the clay catalyst also needs to be done to determine the potential of the sample as a catalyst. It is known that the *h-clay* has a Si/Al mole ratio of 1.79; *Mt-clay* has a Si/Al mole ratio of 1.27 and *c-Mt-clay* has a Si/Al mole ratio of 1.26.

Laser Particle Sizer Analyser Characterisation

The particle size distribution of *h-clay* and *Mt-clay* catalysts may change due to the montmorillonite and separation process (Figure 3). The *h-clay* catalyst is significantly distributed at a particle size of 5.21 µm, accounting for 3.5% of the total samples. After separation and calcination, the particle size distribution increased to 9.60 µm for 4.37% of *Mt-clay* and to 37.86 µm for 9.37% of *c-Mt-clay*. This causes the specific surface area of particles (S) to decrease due to the separation and

calcination process, where the known S values of *h-clay*, *Mt-clay*, and *c-Mt-clay* are 5.57 m² g⁻¹, 1.73 m² g⁻¹ and 0.24 m² g⁻¹ (Table 2). *H-clay* has a particle size distribution of <0.1-2,000.0 µm. While the particle size of *Mt-clay* and *c-Mt-clay* spread over >0.1-2000.0 µm.

The separation and calcination can cause the standard percentile value of the sample to rise (Table 2). The D10 of *h-clay* (0.51 µm) increased in *Mt-clay* (1.54 µm) and *c-Mt-clay* (13.01 µm). This shows that 10% of the samples are below 0.51, 1.54 and 13.01 µm in size. The D50 value of *h-clay* (4.74 µm) increased at *Mt-clay* (9.14 µm) and *c-Mt-clay* (33.01 µm). This indicates that 50% of the samples are smaller than this value for each sample. Similarly, the D90 value becomes 44.14, 54.37 and 83.72 µm in *h-clay*, *Mt-clay* and *c-Mt-clay* which means that 90% of the samples have a small size of that value. The Dav (average particle size) value also increased in *h-clay* 20.75-23.94 µm in *Mt-clay* and 43.02 µm in *c-Mt-clay*. The increase in particle size on the catalysts after separation and calcination may be due to Van der Waals forces increasing the ability for particles to gather to form agglomerations (Hamed et al., 2019).

Mechanism for Separating Montmorillonite from Natural Clay

Montmorillonite mineral was separated from *h-clay* by dispersing it in an NH₄OH solution (Taslimah et al., 2008). NH₄⁺ ions from NH₄OH enter the interlayer of montmorillonite minerals through interlayer cation exchange events, causing swelling in the montmorillonite structure (Gautier et al., 2010; Tong et al., 2021). Swelling that occurs due to intercalation by NH₄⁺ ions can cause the

TABLE 1. CHEMICAL COMPOSITION OF *h-clay*, *Mt-clay*, AND *c-Mt-clay*

Oxide	<i>h-clay</i> (%)	<i>Mt-clay</i> (%)	<i>c-Mt-clay</i> (%)
Al ₂ O ₃	22.854	22.893	25.845
SiO ₂	48.356	34.459	38.502
P ₂ O ₅	3.325	3.261	2.912
K ₂ O	1.108	0.743	0.599
CaO	0.677	0.688	0.597
TiO ₂	2.122	1.866	1.777
V ₂ O ₅	0.069	0.096	0.089
Fe ₂ O ₃	20.476	32.657	28.606
ZnO	0.068	0.119	0.099
SrO	0.005	0.003	0.000
ZrO ₂	0.076	0.101	0.066
Ag ₂ O	0.632	0.675	0.0682
PbO	0.014	0.032	0.024
Si/Al ratio	1.790	1.270	1.260

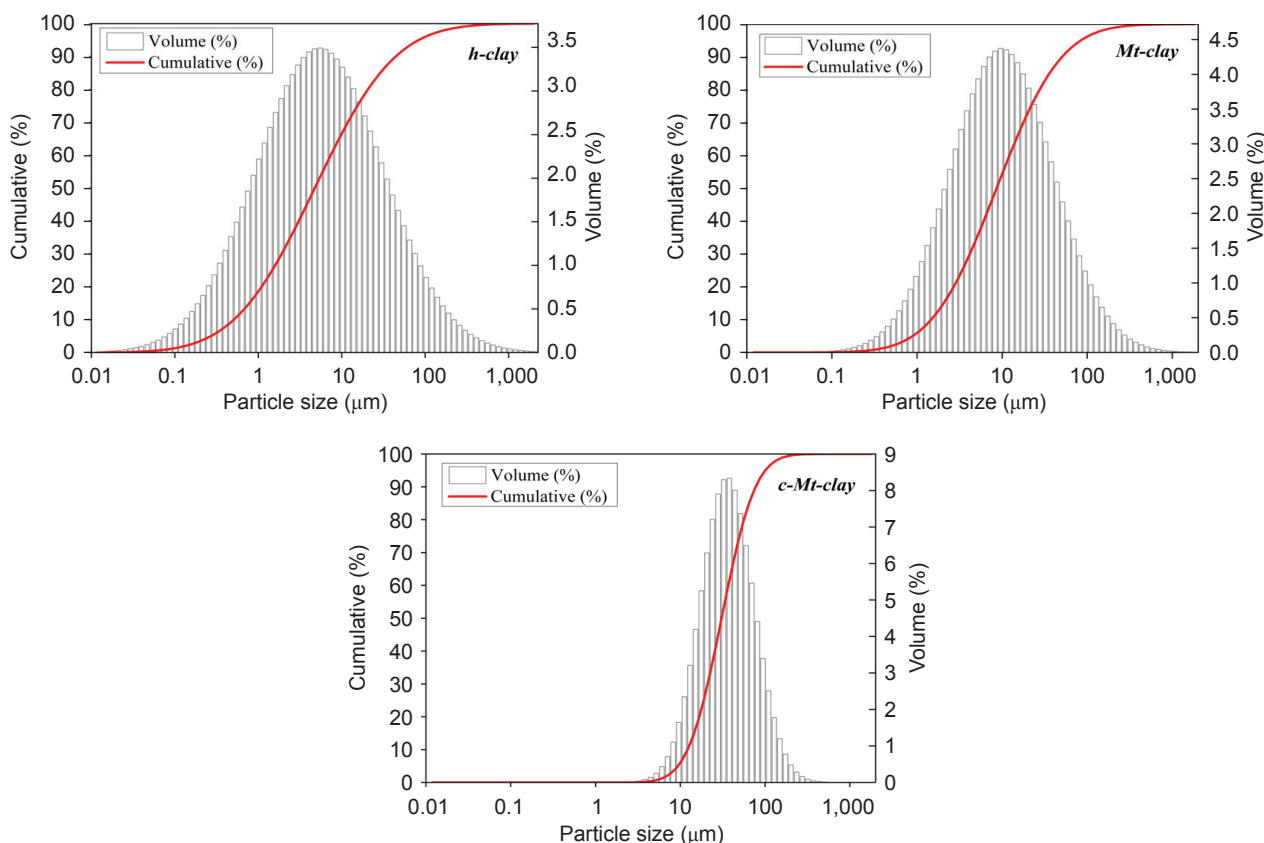


Figure 3. Particle size distribution curves of *h-clay*, *Mt-clay*, and *c-Mt-clay*.

TABLE 2. PARTICLE SIZE DISTRIBUTION CHARACTERISTICS OF *h-clay*, *Mt-clay* AND *c-Mt-clay*

Type of catalyst	D10 (μm)	D50 (μm)	D90 (μm)	Dav (μm)	S ($\text{m}^2 \text{g}^{-1}$)
<i>h-clay</i>	0.51	4.74	44.14	20.75	5.57
<i>Mt-clay</i>	1.54	9.14	54.37	23.94	1.73
<i>c-Mt-clay</i>	13.01	33.01	83.72	43.02	0.24

Note: D10, D50, D90 - standard percentiles; Dav - average particle size (agglomeration size); S - specific surface area of particles.

opening of interlayer space in the montmorillonite structure. The distance between the layers of the montmorillonite structure will increase and eventually release so that the montmorillonite can be dispersed in the NH_4OH solution. In addition, the interaction of NH_4^+ ions with montmorillonite can also increase hydration in montmorillonite (Peng et al., 2020). The separation mechanism of montmorillonite using NH_4OH solution can be seen in Figure 4.

Effect of Separation and Thermal Modification on Mineral Type and Composition

Separation of montmorillonite from *h-clay* has a significant effect on increasing the purity of *Mt-clay*. According to the XRD results, new montmorillonite peaks appear at 2θ : 21.5° and 54.2° . Meanwhile, the peak that existed before separation persists after separation and there is an increase in intensity.

The kaolinite mineral as an impurity in *Mt-clay* also decreased substantially and several peaks experienced a decrease in intensity. Hematite also experiences peak loss. The disappearance of the diffraction peaks of montmorillonite mineral in the *c-Mt-clay* sample calcined at 850°C is due to the dehydroxylation of montmorillonite to meta montmorillonite (Werling et al., 2022). During the calcination process, there is a removal of water from the surface and water between the layers of montmorillonite (Taylor-Lange et al., 2015). This means that montmorillonite undergoes thermal decomposition in the form of dehydration and dehydroxylation during the calcination process (Scrivener & Favier, 2015). According to the XRF results, the Si/Al mole ratio decreased due to the separation and thermal modification processes. A small Si/Al mole ratio indicates a high Al content. High Al comes from aluminate which is negatively charged. The large number of negative charges in

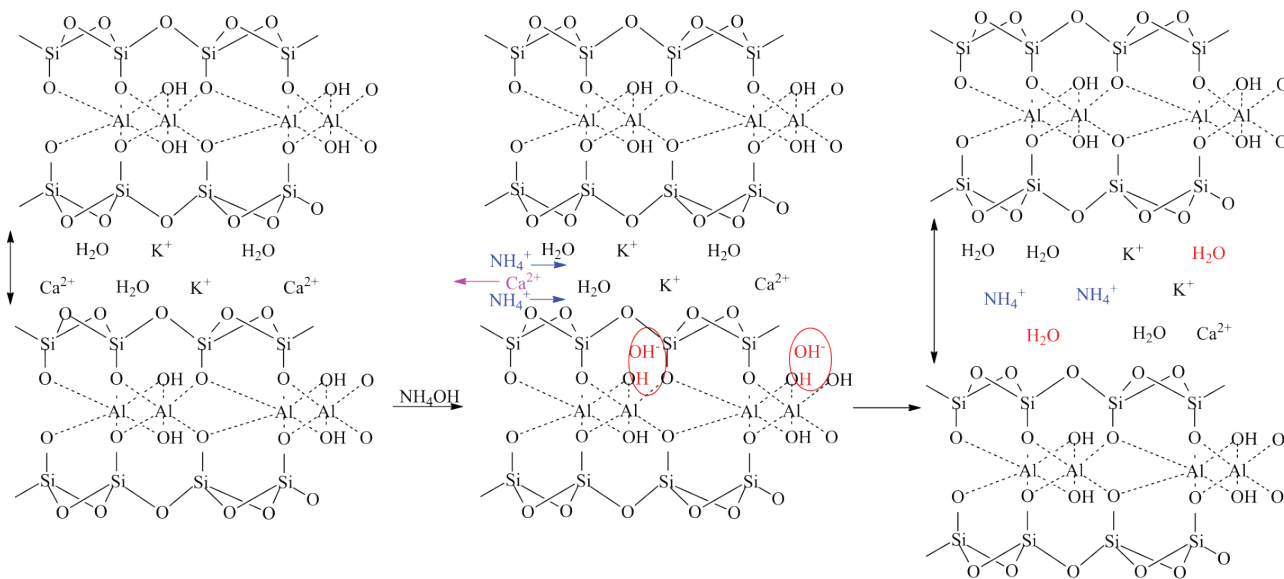


Figure 4. Mechanism of montmorillonite separation using NH_4OH solution.

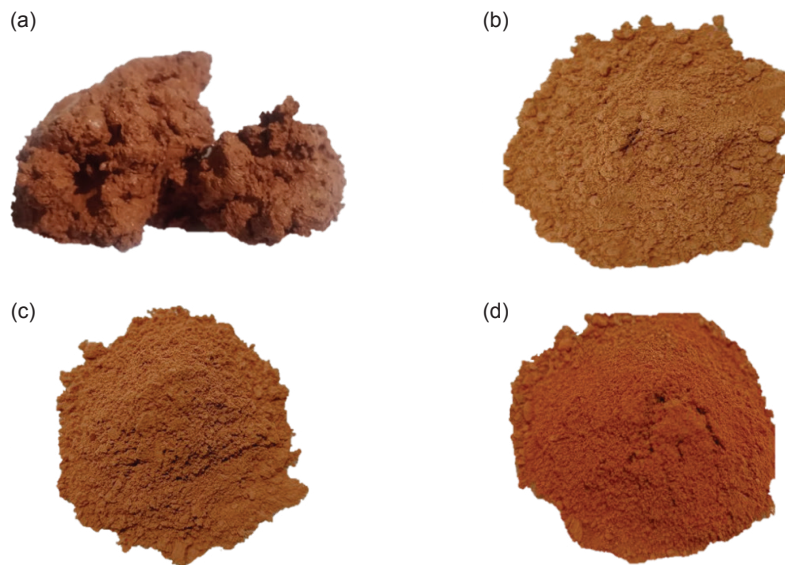


Figure 5. The colour difference of catalyst: (a) n-clay, (b) h-clay, (c) Mt-clay, and (d) c-Mt-clay.

the clay mineral layer will increase the electrostatic interaction with the cations in the clay mineral layer (Strawn, 2021). The change in Si and Al levels in clay is caused by isomorphous substitution in the terrestrial sheet (Kukharenko, 1971). Each catalyst also has a good Si/Al mole ratio (1:2) so that the sample can act as a catalyst. If the Si/Al mole ratio is large (>2), the sample will act as an adsorbent.

Effect of Thermal Separation and Modification on the Physical Properties of the Catalyst

Natural clay which is dark brown (Figure 5a) and becomes light brown (Figure 5b and 5c) in h-clay and Mt-clay. This is due to the loss of adsorbed

water in the clay due to heating at 105°C. The h-clay sample is light brown as shown in the figure. The thermal modification also affects the colour of the catalyst. After coking, c-Mt-clay turned a brick red colour (Figure 5d). The colour change in the clay minerals is due to the transformation of iron oxide contained in each sample. When the clays are calcined in the presence of oxygen at 850°C, goethite [FeO(OH)] transforms into hematite (Fe₂O₃) at 300°C-650°C. Above 650°C, hematite will be reduced to magnetite (Fe₃O₄). However, the samples that have been calcined are cooled again at room temperature. This cooling process will turn magnetite back into hematite. This is what causes the calcined sample to become reddish (Martirena et al., 2020).

Transesterification Reaction Mechanism with Clay Catalyst

The use of each catalyst in the transesterification reaction involves several stages (Figure 6). In the first stage, the negatively charged siloxane surface of the clay mineral catalyst skeleton structure can remove H^+ from the hydroxyl group of methanol to form alcohol anion (methoxide) and adsorb on the cation interlayer. When the reaction occurs, the methoxide anion will attack the carbonyl C atom on the triglyceride molecule to form an intermediate. Then, the intermediate undergoes rearrangement by taking H^+ from the siloxane surface to form methyl esters and diglycerides (Intarapong et al., 2014). These stages occur repeatedly so that three moles of methyl ester and one mole of glycerol are formed from one mole of triglyceride.

Differences in Catalytic Activity

The separation and thermal modification of *Mt-clay* and *c-Mt-clay* catalysts can improve catalytic activity (Figure 7). The yield of biodiesel in the use of *h-clay* catalyst is 57.67%. The use of *Mt-clay* and *c-Mt-clay* catalysts increased the biodiesel yield to 76.20% and 80.11%, respectively. The increase in catalytic activity is due to the decrease in the Si/Al mole ratio according to the XRF results

shown in Table 1. The decrease in the Si/Al mole ratio value indicates the increase in Al content of aluminate which is negatively charged so that its electrostatic interaction with cations in the clay mineral interlayer also increases (Strawn, 2021). This shows that the active site of the catalyst also increases so that it can increase its catalytic activity. According to LPSA results, it turns out that particle size does not contribute to catalytic activity. Although it is generally assumed that catalysts with higher surface areas have better activity, this is not always the case. In some cases, the shape and geometry of the catalyst also play an important role in determining its activity (Großmann et al., 2023).

The catalyst produced in this research is more selective than the clay catalyst used by previous researchers (Febiola et al., 2023; Syukri et al., 2022). The *h-clay*, *Mt-clay*, and *c-Mt-clay* catalysts have high selectivity in producing methyl palmitate and methyl oleate. Meanwhile, previous researchers produced various methyl ester products in each biodiesel. The yield of biodiesel produced in this research is also almost the same as previous research (which chemically modified the clay (Febiola et al., 2023; Kandedo et al., 2009)). This shows that thermal modification with a simple method and lower cost can also increase the catalytic activity of the montmorillonite mineral.

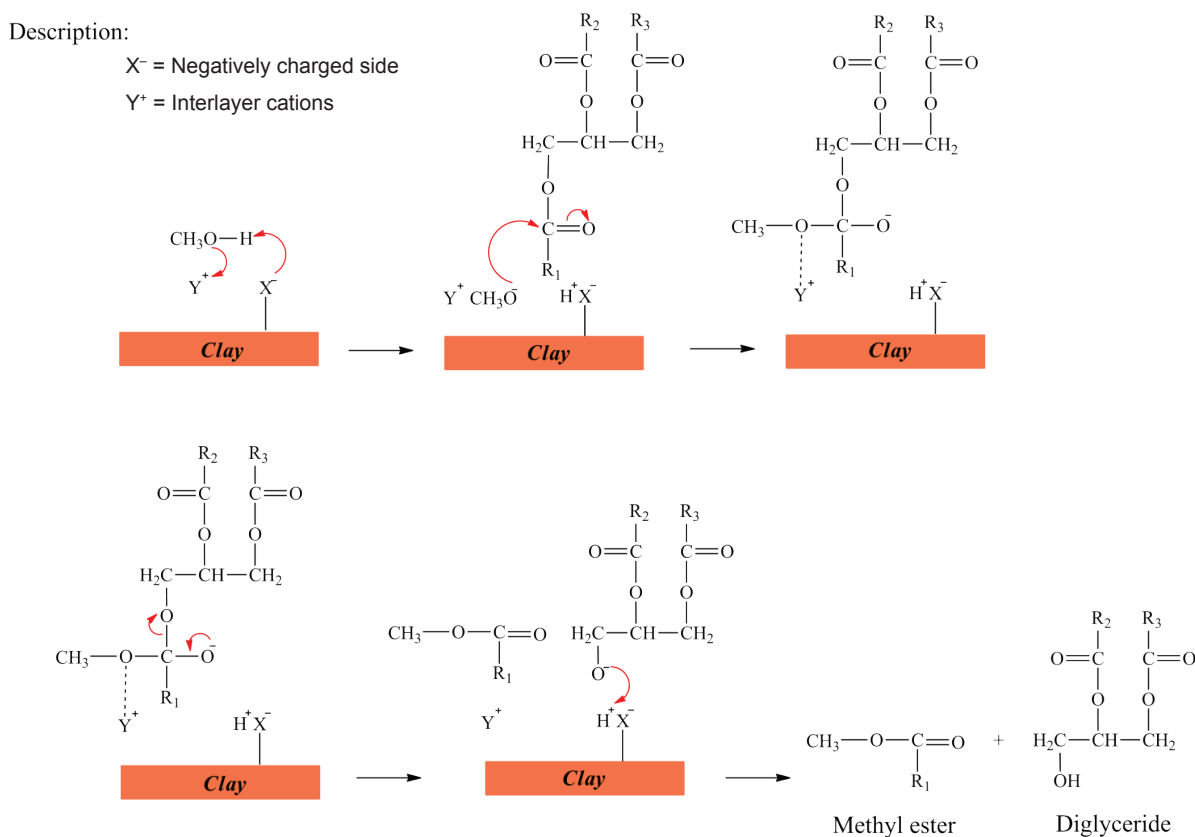


Figure 6. Transesterification reaction mechanism with clay catalysts.

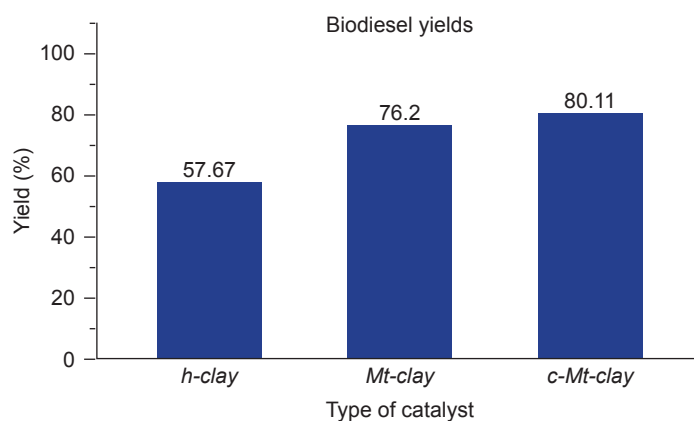


Figure 7. Biodiesel yields catalysed with *h-clay*, *Mt-clay* and *c-Mt-clay*.

TABLE 3. COMPARATIVE STUDY OF MONTMORILLONITE BASED CATALYST ON BIODIESEL YIELD

Catalyst	Feedstock	Temperature (°C)	Time (hr)	Catalyst ratio	Yield (%)	Reference
Cd-Mn-MMT	<i>Prunus cerasoides</i> D. oil	120	5	4.0%	85.00	Munir et al. (2019)
MMT K10	WCO	150	6	4.0%	38.39	Yahya et al. (2020)
Fe-MMT K10	WCO	150	6	4.0%	95.26	Yahya et al. (2020)
Nano-MMT	Crude palm oil	60	3	4.0 g	84.90	Harmawan et al. (2021)
Copper modified MMT	<i>Raphanus raphanistrum</i> L. oil	150	5	3.5%	83.00	Munir et al. (2021)
<i>c-Mt-clay</i>	WFO	70	3	3.0%	80.11	This study

TABLE 4. PHYSICAL PROPERTIES OF BIODIESEL CATALYSED BY *h-clay*, *Mt-clay*, AND *c-Mt-clay*

Properties	Standards	Type of catalyst		
		<i>h-clay</i>	<i>Mt-clay</i>	<i>c-Mt-clay</i>
Density (g cm ⁻³)	0.86-0.90 (ASTM D6751)	0.87	0.86	0.86
Water content (%)	0.05 (ASTM D2709)	0.47	0.03	0.02

Transesterification reactions produce similar methyl esters, namely methyl palmitate and methyl oleate. Methyl palmitate is a saturated methyl ester, while methyl oleate is an unsaturated methyl ester. Saturated methyl esters are the most desirable component in biodiesel. This is related to their stability against oxidation. Unsaturated methyl esters, on the other hand, are more easily oxidised and will form gum in the fuel which can cause fuel corrosion (Lucchini et al., 2011).

Based on the comparison of montmorillonite-based catalyst studies in the Table 3, the yield obtained from this study is higher than the yield obtained in other studies using the MMT K10 synthetic catalyst without treatment and modification. However, when compared with montmorillonite catalysts that were modified by making them nanostructured or by imposition of metal, the yield values obtained in this study were relatively lower.

Physical Properties of Biodiesel Products

The physical properties of the biodiesel product determined are density and water content (Table 4). Based on ASTM D6751, biodiesel has a density of 0.86-0.90 g cm⁻³ at 15°C, while the maximum water content in biodiesel is 0.05% (ASTM D2709). The transesterification reaction products catalysed by *h-clay*, *Mt-clay* and *c-Mt-clay* have densities of 0.87, 0.86 and 0.86 g cm⁻³, respectively. While the water content in *h-clay*, *Mt-clay* and *c-Mt-clay* biodiesel products is 0.47%, 0.03% and 0.02%, respectively. Therefore, biodiesel products catalysed by *Mt-clay* and *c-Mt-clay* are included in the biodiesel group because the values meet with the density and water content under ASTM. While the product catalysed by *h-clay* is not considered biodiesel because the water content exceeds the maximum limit set by ASTM.

CONCLUSION

This research has succeeded in separating the mineral montmorillonite from the natural clay of Tanah Datar. Calcined montmorillonite caused changes in the constituent phases, and the element levels, as well as the oxide levels contained therein. All catalysts contain the main elements of Si, Al, and Fe. Separation and thermal modification caused changes in elemental content and Si/Al mole ratio from 1.79 in *h-clay* down to 1.27 and 1.26 in *Mt-clay* and *c-Mt-clay* samples. Thermal treatment of *c-Mt-clay* caused colour changes from light brown to brick red. Montmorillonite turned into meta montmorillonite after calcined at 850°C. Particle size does not contribute to catalytic activity. Separation and thermal modification of *Mt-clay* and *c-Mt-clay* catalysts can increase biodiesel yield. The *h-clay* catalyst had a biodiesel yield of 57.67%, which increased to 76.20% in the *Mt-clay* catalyst and 80.11% in the *c-Mt-clay* catalyst. Therefore, we suggest that other researchers can use this method to produce a good catalyst for producing biodiesel.

ACKNOWLEDGEMENT

We expressed our best gratitude for funding from LPPM Universitas Andalas with Research Contract No. T/174/UN.16.17/PT.01.03/IS-RPT/2022. September 28, 2022.

REFERENCES

- Abdrakhimova, E. S., & Abdrakhimov, V. Z. (2007). Synthesis of mullite from technogenic materials and pyrophyllite. *Russian Journal of Inorganic Chemistry*, 52(3), 345–350. <https://doi.org/10.1134/S0036023607030096>
- Admi, A., Angellika, F. T., Rilda, Y., & Syukri, S. (2022). Pengaruh modifikasi fisika pada komposisi, struktur kristal dan sifat katalitik Lempung Solok [The effect of physical modification on the composition, crystal structure and catalytic properties of Solok clay]. *Jurnal Fisika Unand*, 11(4), 548–555. <https://doi.org/10.25077/jfu.11.4.548-555.2022>
- Azni, M. A., Md Khalid, R., Hasran, U. A., & Kamarudin, S. K. (2023). Review of the effects of fossil fuels and the need for a hydrogen fuel cell policy in Malaysia. *Sustainability*, 15(5), Article 4033. <https://doi.org/10.3390/su15054033>
- Bambase, M. E., Almazan, R. A. R., Demafelis, R. B., Sobremisana, M. J., & Dizon, L. S. H. (2021). Biodiesel production from refined coconut oil using hydroxide-impregnated calcium oxide by cosolvent method. *Renewable Energy*, 163, 571–578. <https://doi.org/10.1016/j.renene.2020.08.11>
- Belghazdis, M., & Hachem, E. K. (2022). Clay and clay minerals: A detailed review. *International Journal of Recent Technology and Applied Science*, 4(2), 54–75. <https://doi.org/10.36079/lamintang.ijortas-0402.367>
- Bibin, C., Gopinath, S., Aravindraj, R., Devaraj, A., Gokula Krishnan, S., & Jeevaanathan, J. K. S. (2020). The production of biodiesel from castor oil as a potential feedstock and its usage in compression ignition engine: A comprehensive review. *Materials Today: Proceedings*, 33, 84–92. <https://doi.org/10.1016/j.matpr.2020.03.205>
- Faruque, M. O., Razzak, S. A., & Hossain, M. M. (2020). Application of heterogeneous catalysts for biodiesel production from microalgal oil – A review. *Catalysts*, 10(9), 1–25. <https://doi.org/10.3390/catal10091025>
- Febiola, F., Rahmayeni, Admi, & Syukri. (2023). Kaolinite and illite based clay supporting nickel: Its synthesis, characterization, and catalytic optimization in a lab-scale fatty acid methyl ester production. *Herald of the Bauman Moscow State Technical University. Series Natural Sciences*, 4(109), 159–174. <https://doi.org/10.18698/1812-3368-2023-4-159-174>
- Febrianto, F., Setianingsih, A., & Riyani, A. (2020). Determination of free fatty acid in frying oils of various foodstuffs. *Indonesian Journal of Chemistry and Environment*, 2(1), 1–6. <https://doi.org/10.21831/ijce.v2i1.30288>
- Gaide, I., Makareviciene, V., Sendzikiene, E., & Kazancev, K. (2023). Snail shells as a heterogeneous catalyst for biodiesel fuel production. *Processes*, 11(1), Article 260. <https://doi.org/10.3390/pr11010260>
- Gautier, M., Muller, F., Le Forestier, L., Beny, J. M., & Guegan, R. (2010). NH₄-smectite: Characterization, hydration properties and hydro mechanical behaviour. *Applied Clay Science*, 49(3), 247–254. <https://doi.org/10.1016/j.clay.2010.05.013>
- Gouran, A., Aghel, B., & Nasirmanesh, F. (2021). Biodiesel production from waste cooking oil using wheat bran ash as a sustainable biomass. *Fuel*, 295, Article 120542. <https://doi.org/10.1016/j.fuel.2021.120542>

- Götze, J., Pan, Y., & Müller, A. (2021). Mineralogy and mineral chemistry of quartz: A review. *Mineralogical Magazine*, 85(5), 639–664. <https://doi.org/10.1180/mgm.2021.72>
- Großmann, P. F., Tonigold, M., Szesni, N., Fischer, R. W., Seidel, A., Achterhold, K., Pfeiffer, F., & Rieger, B. (2023). Influence of internal and external surface area on impregnation and activity of 3D printed catalyst carriers. *Catalysis Communications*, 175, Article 106610. <https://doi.org/10.1016/j.catcom.2023.106610>
- Hamed, N., El-Feky, M. S., Kohail, M., & Nasr, E. S. A. R. (2019). Effect of nano-clay de-agglomeration on mechanical properties of concrete. *Construction and Building Materials*, 205, 245–256. <https://doi.org/10.1016/j.conbuildmat.2019.02.018>
- Harmawan, T., Ani, W., Andani, P., & Fadlly, T. A. (2021). Production of biodiesel through transesterification of crude palm oil (CPO) using montmorillonite nanoparticles (Nano-MMT) as heterogeneous solid catalyst. *Proceedings of the 2nd International Conference on Science and Technology in Modern Society (ICSTMS 2020)*, 576, 69–72.
- Intarapong, P., Jindavat, C., Luengnaruemitchai, A., & Jai-In, S. (2014). The transesterification of palm oil using KOH supported on bentonite in a continuous reactor. *International Journal of Green Energy*, 11, 987–1001. <https://doi.org/10.1080/15435075.2013.829477>
- Irawan, B., Rusdianasari, & Hasan, A. (2021). Pyrolysis process of fatty acid methyl ester (FAME) conversion into biodiesel. *International Journal of Research and Vocational Studies*, 1(2), 1–10.
- Jabbari, H. (2018). Production of methyl ester biofuel from sunflower oil via transesterification reaction. *Asian Journal of Nanoscience and Materials*, 1(2), 52–55. <https://doi.org/10.26655/AJNANOMAT.2018.3.1>
- Kansedo, J., Lee, K. T., & Bhatia, S. (2009). Biodiesel production from palm oil via heterogeneous transesterification. *Biomass and Bioenergy*, 33(2), 271–276. <https://doi.org/10.1016/j.biombioe.2008.05.011>
- Khan, E., Ozaltin, K., Spagnuolo, D., Bernal-Ballen, A., Piskunov, M. V., & Di Martino, A. (2023). Biodiesel from rapeseed and sunflower oil: Effect of the transesterification conditions and oxidation stability. *Energies*, 16(2), 1–13. <https://doi.org/10.3390/en16020657>
- Kibar, M. E., Hilal, L., Çapa, B. T., Bahçivanlar, B., & Abdeljelil, B. (2023). Assessment of homogeneous and heterogeneous catalysts in transesterification reaction: A mini review. *ChemBioEng Reviews*, 10(4), 412–422. <https://doi.org/10.1002/cben.202200021>
- Kukhareenko, A. A. (1971). The problem of isomorphism in mineralogy. *International Geology Review*, 13(4), 546–557. <https://doi.org/10.1080/00206817109475467>
- Lomertwala, H. M., Njoroge, P. W., Opiyo, S. A., & Ptoton, B. M. (2019). Characterization of clays from selected sites for refractory application. *International Journal of Scientific Research and Publications*, 9(11), Article p9581. <https://doi.org/10.29322/IJSRP.9.11.2019.P9581>
- Lucchini, V., Fabris, M., Noè, M., Perosa, A., & Selva, M. (2011). Kinetic parameter estimation of solvent-free reactions monitored by ^{13}C NMR spectroscopy, a case study: Mono- and di-(hydroxy)ethylation of aniline with ethylene carbonate. *International Journal of Chemical Kinetics*, 43(3), 154–160. <https://doi.org/10.1002/kin.20532>
- Lugo-Méndez, H., Sánchez-Domínguez, M., Sales-Cruz, M., Olivares-Hernández, R., Lugo-Leyte, R., & Torres-Aldaco, A. (2021). Synthesis of biodiesel from coconut oil and characterization of its blends. *Fuel*, 295(1), Article 120595. <https://doi.org/10.1016/j.fuel.2021.120595>
- Martirena, F., Almenares, R., Zunino, F., Alujas, A., & Scrivener, K. (2020). Color control in industrial clay calcination. *RILEM Technical Letters*, 5, 1–7. <http://doi.org/10.21809/rilemtechlett.2020.107>
- Mishra, V. K., & Goswami, R. (2018). A review of production, properties and advantages of biodiesel. *Biofuels*, 9(2), 273–289. <https://doi.org/10.1080/17597269.2017.1336350>
- Munir, M., Ahmad, M., Waseem, A., Zafar, M., Saeed, M., Wakeel, A., Nazish, M., & Sultana, S. (2019). Scanning electron microscopy leads to identification of novel nonedible oil seeds as energy crops. *Microscopy Research and Technique*, 82(7), 1165–1173. <https://doi.org/10.1002/jemt.23265>
- Munir, M., Ahmad, M., Rehan, M., Saeed, M., Lam, S. S., Nizami, A. S., Waseem, A., Sultana, S., & Zafar, M. (2021). Production of high quality biodiesel from novel non-edible *Raphanus raphanistrum* L. seed oil using copper

- modified montmorillonite clay catalyst. *Environmental Research*, 193, Article 110398. <https://doi.org/10.1016/j.envres.2020.110398>
- Mustafa, N., Zubair, M., Uddin, N., Ali, S., Haider, A., & Badshah, A. (2023). Catalytic conversion of castor oil into biodiesel by triorganotin(IV) catalysts: Chromatographic and spectroscopic characterization with theoretical support. *Proceedings of the Pakistan Academy of Sciences. Part B. Life and Environmental Sciences*, 60(2), 225–232. [https://doi.org/10.53560/PPASB\(60-2\)816](https://doi.org/10.53560/PPASB(60-2)816)
- Nang, H. L. L., Wafti, N. S. A., & May, C. Y. (2009). Production technology of biodiesel from palm fatty acid distillate (PFAD). *MPOB Information Series*, 471. MPOB
- Negm, N. A., Sayed, G. H., Yehia, F. Z., Habib, O. I., & Mohamed, E. A. (2017). Biodiesel production from one-step heterogeneous catalyzed process of castor oil and jatropha oil using novel sulphonated phenyl silane montmorillonite catalyst. *Journal of Molecular Liquids*, 234, 157–163. <https://doi.org/10.1016/j.molliq.2017.03.043>
- Nguyen, V. G., Pham, M. T., Le, N. V. L., Le, H. C., Truong, T. H., & Cao, D. N. (2023). A comprehensive review on the use of biodiesel for diesel engines. *International Journal of Renewable Energy Development*, 12(4), 720–740.
- Pacheco-López, A., Lechtenberg, F., Somoza-Tornos, A., Graells, M., & Espuña, A. (2021). Economic and environmental assessment of plastic waste pyrolysis products and biofuels as substitutes for fossil-based fuels. *Frontiers in Energy Research*, 9, 1–14. <https://doi.org/10.3389/fenrg.2021.676233>
- Palaniselvam, V., Rajan, S. S., Sriramajaman, S., & Ramesh, D. (2024). Effect of reaction time on various properties of palm oil biodiesel in continuous biodiesel reactor. *Journal of Oil Palm Research*, 36(2), 484–494. <https://doi.org/10.21894/jopr.2023.0040>
- Park, J. H., Shin, H. J., Kim, M. H., Kim, J. S., Kang, N., Lee, J. Y., Kim, K. T., Lee, J. I., & Kim, D. D. (2016). Application of montmorillonite in bentonite as a pharmaceutical excipient in drug delivery systems. *Journal of Pharmaceutical Investigation*, 46(4), 363–375. <https://doi.org/10.1007/s40005-016-0258-8>
- Pasae, Y., Melawaty, L., Ruswanto, Bulu, L., & Allo, E. L. (2021). Effectiveness of heterogenous catalyst in biodiesel production process: The use of zeolite, ZnO and Al₂O₃. *Journal of Physics: Conference Series*, 1899(1), Article 012032. <https://doi.org/10.1088/1742-6596/1899/1/012032>
- Peng, C., Wang, G., Qin, L., Luo, S., Min, F., & Zhu, X. (2020). Molecular dynamics simulation of NH₄-montmorillonite interlayer hydration: Structure, energetics, and dynamics. *Applied Clay Science*, 195, Article 105657. <https://doi.org/10.1016/j.clay.2020.105657>
- Pikula, K., Zakharenko, A., Stratidakis, A., Razgonova, M., Nosyrev, A., Mezhuev, Y., Tsatsakis, A., & Golokhvast, K. (2020). The advances and limitations in biodiesel production: Feedstocks, oil extraction methods, production, and environmental life cycle assessment. *Green Chemistry Letters and Reviews*, 13(4), 11–30. <https://doi.org/10.1080/17518253.2020.1829099>
- Rehman, A., Ma, H., Chishti, M. Z., Ozturk, I., Irfan, M., & Ahmad, M. (2021). Asymmetric investigation to track the effect of urbanization, energy utilization, fossil fuel energy and CO₂ emission on economic efficiency in China: Another outlook. *Environmental Science and Pollution Research*, 28(14), 17319–17330. <https://doi.org/10.1007/s11356-020-12186-w>
- Salaheldeen, M., Mariod, A. A., Aroua, M. K., Rahman, S. M. A., Soudagar, M. E. M., & Fattah, I. M. R. (2021). Current state and perspectives on transesterification of triglycerides for biodiesel production. *Catalysts*, 11(9), Article 1121. <https://doi.org/10.3390/catal11091121>
- Scrivener, K., & Favier, A. (2015). *Calcined clays for sustainable concrete* (pp. 117–124). RILEM Bookseries.
- Shapkin, N. P., Leont'ev, L. B., Khal'chenko, I. G., Panasenko, A. E., Maiorov, V. Y., Razov, V. I., Kaidalova, T. A., & Papynov, E. K. (2017). Chemical modification of natural clays. *Russian Journal of Inorganic Chemistry*, 62(9), 1209–1214. <https://doi.org/10.1134/S0036023617090121>
- Sharma, P., & Bhavani, A. G. (2021). Green, cost effective barium loaded montmorillonite catalyst for biodiesel synthesis from waste cooking oil. *Materials Today: Proceedings*, 45, 4544–4549. <https://doi.org/10.1016/j.matpr.2020.12.1202>
- Siddeg, A. B., Adam, U., Jaat, N., Khalid, A., Sapit, A., Mohd, S., & Abd. Jalal, M. (2022). Analysis of the influences of biodiesel on performance

- and emissions of a diesel engine. *Journal of Automotive Powertrain and Transport Technology*, 2(2), 1–8.
- Silva, A. A. de L., Periera, M. G. A., Souza, L. Di, & Caldeira, A. G. D. S. (2015). Iodeto de potássio suportado em MCM-41 como catalisador para síntese de biodiesel utilizando micro-ondas [Potassium iodide supported on MCM-41 as a catalyst for biodiesel synthesis using microwaves]. *Blucher Chemical Proceedings*, 537–545.
- Strawn, D. G. (2021). Sorption mechanisms of chemicals in soils. *Soil Systems*, 5(1), Article 13. <https://doi.org/10.3390/soilsystems5010013>
- Sukkathanyawat, H., & Wichianwat, K. (2023). Optimisation of FAME production from waste cooking palm oil with KOH catalyst supported on palm kernel shells ash (PKSA) using response surface methodology (RSM). *Journal of Oil Palm Research*, 35(4), 668–681. <https://doi.org/10.21894/jopr.2023.0005>
- Supriyanto, E., Sentanuhady, J., Dwiputra, A., Permana, A., & Muflikhun, M. A. (2021). The recent progress of natural sources and manufacturing process of biodiesel: A review. *Sustainability*, 13(10), Article 5599. <https://doi.org/10.3390/su13105599>
- Suwarno, Rohana, & Indra Siregar, I. (2021). Study feasibility analysis of biodiesel energy processing used cooking oil. *Budapest International Research and Critics Institute Journal*, 4(3), 7374–7386.
- Syukri, Febiola, F., Rahmayeni, Mai, E., Yulia P., & Upita, S. (2022). Effect of thermal treatment and nickel-salt modification on the catalytic performance of the illite-kaolinite clay from Bukittinggi of West Sumatra in palm oil transesterification. *Herald of the Bauman Moscow State Technical University. Series Natural Sciences*, 2, 125–136.
- Syukri, S., Septioga, K., Arief, S., Putri, Y. E., Efdi, M., & Septiani, U. (2020). Natural clay of Pasaman Barat enriched by CaO of chicken eggshells as catalyst for biodiesel production. *Bulletin of Chemical Reaction Engineering and Catalysis*, 15(3), 662–673. <https://doi.org/10.9767/brec.15.3.8097.662-673>
- Takabatake, M., & Motokura, K. (2022). Montmorillonite-based heterogeneous catalysts for efficient organic reactions. *Nano Express*, 3(1), Article 014004. <https://doi.org/10.1088/2632-959X/ac5ac3>
- Taslimah, Kusumawardani, R., & Azmiyawati, C. (2008). Pilarisasi lempung dengan Al₂O₃ untuk agen pemucat minyak sawit [Pillaring of clay with Al₂O₃ for palm oil bleaching agent]. *Jurnal Kimia Sains dan Aplikasi*, 11(2), 48–51.
- Taylor-Lange, S. C., Lamon, E. L., Riding, K. A., & Juenger, M. C. G. (2015). Calcined kaolinite-bentonite clay blends as supplementary cementitious materials. *Applied Clay Science*, 108, 84–93. <https://doi.org/10.1016/j.clay.2015.01.025>
- Tong, K., Guo, J., Chen, S., Yu, F., Li, S., & Dai, Z. (2021). A simulation study on the swelling and shrinking behaviors of nanosized montmorillonite based on Monte Carlo and molecular dynamics. *Geofluids*, 2021, Article 1038205. <https://doi.org/10.1155/2021/1038205>
- Tripol'Skaya, T. A., Pilipenko, G. P., Legurova, E. A., Pokhabova, I. V., & Prikhodchenko, P. V. (2009). New peroxo derivatives of synthetic montmorillonite structures. *Russian Journal of Inorganic Chemistry*, 54(4), 512–516. <https://doi.org/10.1134/S0036023609040044>
- Ubaid, H. S., Noureen, S., Razzaq, I., Alkhter, S., Mehmood, F., Razzaq, Z., & Jabeen, M. (2022). Optimisation and characterisation of acid catalysed castor biodiesel and its blends. *Journal of the Turkish Chemical Society, Section A: Chemistry*, 9(4), 1007–1022. <https://doi.org/10.18596/jotcsa.1116677>
- Uddin, F. (2018). Montmorillonite: An introduction to properties and utilization. In M. Zoveidavianpoor (Ed.), *Current topics in the utilization of clay in industrial and medical applications* (pp. 1–202). IntechOpen.
- Vital-López, L., Mercader-Trejo, F., Rodríguez-Reséndiz, J., Zamora-Antuñano, M. A., Rodríguez-López, A., Esquerre-Verastegui, J. E., Farrera Vázquez, N., & García-García, R. (2023). Electrochemical characterization of biodiesel from sunflower oil produced by homogeneous catalysis and ultrasound. *Processes*, 11(1), Article 94. <https://doi.org/10.3390/pr11010094>
- Werling, N., Kaltenbach, J., Weidler, P. G., Schuhmann, R., Dehn, F., & Emmerich, K. (2022). Solubility of calcined kaolinite, montmorillonite, and illite in high molar NaOH and suitability as precursors for geopolymers. *Clays and Clay Minerals*, 70(2), 270–289. <https://doi.org/10.1007/s42860-022-00185-6>

- Wu, Z., Zhao, H., Zhou, X., Wang, Y., Zuo, K., & Cheng, H. (2022). Thermal migration behavior of Na⁺, Cu²⁺ and Li⁺ in montmorillonite. *Minerals*, 12(4), Article 477. <https://doi.org/10.3390/min12040477>
- Xu, H., Ou, L., Li, Y., Hawkins, T. R., & Wang, M. (2022). Life cycle greenhouse gas emissions of biodiesel and renewable diesel production in the United States. *Environmental Science & Technology*, 56(12), 7512–7521. <https://doi.org/10.1021/acs.est.2c00289>
- Yaghmaeiyan, N., Mirzaei, M., & Delghavi, R. (2022). Montmorillonite clay: Introduction and evaluation of its applications in different organic syntheses as catalyst: A review. *Results in Chemistry*, 4, Article 100549. <https://doi.org/10.1016/j.rechem.2022.100549>
- Yahya, S., Muhamad Wahab, S. K., & Harun, F. W. (2020). Optimization of biodiesel production from waste cooking oil using Fe-Montmorillonite K10 by response surface methodology. *Renewable Energy*, 157, 164–172. <https://doi.org/10.1016/j.renene.2020.04.149>